JOURNAL OF OPTOELECTRONICS AND ADVNACDE MATERIALS Vol. 8, No. 2, April 2006, p. 794 - 799

Electrical and photoelectrical properties of vacuum deposited Se-Te-Pb thin films

N. KUSHWAHA, R. K. SHUKLA, A. KUMAR*
Department of Physics, Harcourt Butler Technological Institute, Kanpur-208 002, India

The d. c. electrical properties of amorphous thin films of $Se_{85}Te_{15-x}Pb_x$, prepared by vacuum deposition technique, have been studied at low and at relatively high temperatures. The dark conductivity studies show that the conductivity increases with increasing temperature at all temperature range. Two types of conduction mechanisms were found to dominate in the measured temperature range, namely band conduction through extended states (which dominates at the intermediate-temperature region) and hopping around the Fermi level (which dominates at the low-temperature region). At low temperature, the density of states and other related Mott's parameters are calculated near the Fermi level. A discontinuity, found in the curve at high temperature may be explained due to structural changes that occur near glass transition temperature. Transient photoconductivity measurements at different temperatures and intensities indicate that the decay of photoconductivity is quite slow. Thin films exhibit long-lived residual photoconductivity, called persistent photoconductivity, with an extremely slow decay rate. The persistent photoconductivity increases with an increase in intensity. Photoconductivity decay, even after subtraction of persistent photoconductivity, is found to be non - exponential suggest the presence of continuously distributed deep localised gap states in this material. Differential lifetime and carrier lifetime are also calculated.

(Received January 21, 2006; accepted March 23, 2006)

Keywords: Chalcogenide glasses, photoconductivity, Mott's parameters, Density of defect states, Low temperature conductivity

1. Introduction

There is a striking range of novel phenomena which occur in non-oxide glasses, especially the chalcogenides (S, Se, Te), either in elemental form or alloyed with atoms from columns III, IV or V. The materials tend to have similar electronic state densities, possessing an optical gap of about 2 eV and exponential band tails at both band edges. They also have the important property that, although there are some gap states, they do not carry the traditional Electron Spin Resonance defect signature of unpaired spins. The lone-pair character of both the conduction and valence tails leads to very rich behaviour under the influence of light [1].

The current interest on the chalcogenide glasses is on X-ray imaging and photonics [2]. These materials are technologically important. For example, a-Se is a classic material for xerographic applications [3], and has recently been highlighted as a promising photoconductive material for digital X-ray radiography [1]. A new frontier, which has only just begun to attract interest, is a thermal optical micro fabrication (micrometer length scale deformations can be accomplished via light exposure); this approach has already been used to make optical gratings and micro lenses [4, 5]. The structure of the thin films strongly influences the electronic properties and is highly dependent upon the preparation technique and deposition conditions. These semiconductors chalcogenide glasses also exhibit many interesting properties, such as photodarkening, photodoping, photocrystallization and photoconductivity. The photoconductivity of these glasses is very helpful in understanding the phenomenon of recombination kinetics, and the nature and distribution of localized states in the forbidden energy gap. Moreover, the photosensitivity and photogeneration of the charge carriers and their transport in the medium can also be determined.

In previous papers [6,7] we have investigated the $Se_{100-x}Te_x$ and $Se_{70}Te_{30-x}Cd_x$ amorphous films and observed the Meyer-Neldel rule is obeyed in both cases. The electrical analysis of Pb-based chalcogenides is very useful because of the charge reversal from *p*-type to *n*-type in Ge–Se–Pb system [8] is observed in spite of the usual *p*-type charge carrier in the chalcogenide glasses. Charge reversal is also found in Se–In–Pb system [9].

However, few attempts have been made [10-13] to the study of chalcogenide glasses with one of the element as Pb. It may be due to the fact that lead is the last element in radioactive series, which is most stable, or lead is one with which it is most difficult to form a glass. The differential scanning calorimetric study [12] and the optical properties [14] have been reported on the $Se_{85}Te_{15-x}Pb_x$ glassy alloys

In view of this, the study of the electrical and photoelectrical properties of the $Se_{85}Te_{15-x}Pb_x$ (x = 2, 4& 6) thin films are carried out over a wide temperature range and the results are reported. Section 2 describes the experimental details. The results have been presented and discussed in section 3. The conclusions have been presented in the last section.

2. Experimental

Glassy alloys of $Se_{85}Te_{15-x}Pb_x$ (x = 2, 4 & 6) were prepared from the melt by the quenching technique. The bulk material was prepared by mixing 99.999% pure powders of selenium, Tellurium and lead. The mixture was sealed in a quartz ampoule at a pressure of 10^{-5} Torr and melted at 900 °C. During heating, all the ampoules were constantly rocked, by rotating a ceramic rod to which the ampoules were tucked away in the furnace for 10 hours and the ampoule was rotated slowly at a rate of 3-4 °C/min for homogeneous mixing. The melts were cooled rapidly by removing the ampoules from the furnace and dropping them to ice-cooled water.

Thin films of these glasses were prepared by vacuum evaporation technique keeping glass substrates at room temperature. Vacuum evaporated indium electrodes at bottom were used for the electrical contact. The thickness of the films was ~ 500 nm. The co-planar structure (length ~ 1.2 cm and electrode separation ~ 0.5 mm) was used for the present measurements.

For the measurement of electrical conductivity & transient photoconductivity, thin film samples were mounted in a specially designed sample holder which has a transparent window to shine light for these measurements in a vacuum ~10^{-3} Torr. The temperature of the films was controlled by mounting a heater inside the sample holder and measured by a calibrated copper - constantan thermocouple mounted very near to the films. The low temperature was obtained by cooling the samples using liquid nitrogen

The source of light was a 200 W tungsten lamp. The intensity of light was varied by changing the voltage across the lamp. The intensity was measured by a lux-meter. The d. c. current is measured by a digital Electrometer (Keithley, model 614). The heating rate is kept quite small (0.5 K/min) for these measurements.

Before measuring the dark conductivity, the films were first annealed below glass transition temperature T_g for two hours in a vacuum ~ 10^{-3} Torr. I-V characteristics are found to be linear and symmetric up to 30 V in all the glasses studied. The present measurements are, however, made by applying only 10 V across the films.

3. Results and discussion

The electrical conductivity of the $Se_{85}Te_{15-x}Pb_x$ thin films have been measured in the temperature range 230 K to 320 K in dark and a plot of lnσ versus 10^3/T is shown in Fig. 1a. Figure shows that there exist three different regions in the range 230 K to 320 K. One such region is at low temperatures 230 K to 250 K and two regions are in high temperature range 250 K to 320 K. The change in nature of slope near 300 K may be due to appearance of glass transition temperature (310 K).

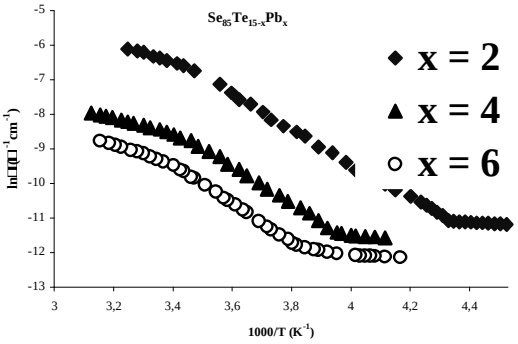

Fig. 1a. Temperature dependence of conductivity plotted as lnσ vs 1000/T in a- $Se_{85}Te_{15-x}Pb_x$ thin film.

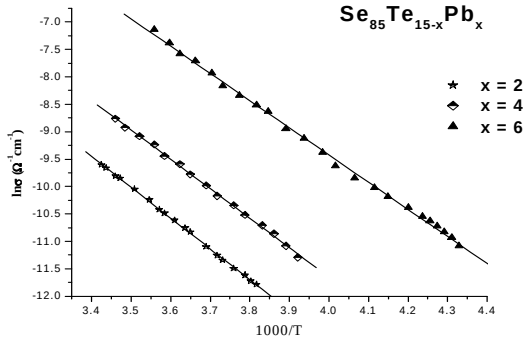

Fig. 1b. As lnσ vs 1000/T in the temperature range where the Arhenious behaviour is observed as well as the linear fit.

From 250 K to 300 K, the Arrhenius behaviour is observed where conductivity increases exponentially with temperature following the relation:

$$\sigma = \sigma_0 \exp(-\Delta E / k T) \qquad (1)$$

where ΔE is the activation energy for conduction and k is the Boltzmann's constant.

The ln σ vs. 1000/T curves for a- $Se_{85}Te_{15-x}Pb_x$ thin films separately plotted in Fig. 1b in the intermediate temperature range where the conductivity shows the Arrhenius behaviour with a single slope. In the above temperature range, the exponential variation of conductivity with temperature indicates that the conductivity in these glasses is due to a thermally activated process. The values of conductivity σ at a particular temperature 265 K, pre-exponential factor σ_0 and ΔE for different compositions of $Se_{85}Te_{15-x}Pb_x$ glassy alloys are given in Table 1. It is clear from the Table that the conductivity increases as Pb concentration increases and the activation energy decreases with addition of Pb to the Se-Te system. This may be attributed to enhanced valence band tailing with Pb incorporation. Similar results have been reported for Pb addition to $Se_{80}Te_{20}$ matrix [10]. The optical energy gap reported for same compositions show that activation energy and optical energy gap follow the same trend with different compositions of Pb. The

magnitude of σ_0 lies in the range of 10^3-10^4 ohm^{-1}cm^{-1} which indicates that the conduction is due to the carriers excited into the extended states [14].

Table 1. D.C. conduction parameters in the high temperature range.

$Se_{85}Te_{15-x}Pb_x$ x at (%)	σ (ohm^{-1}cm^{-1}) at 265 K	ΔE (eV)	σ_0 (ohm^{-1}cm^{-1})
2	1.20×10^{-5}	0.49 ± 0.003	2.5×10^{4}
4	3.22×10^{-5}	0.45 ± 0.005	6.1×10^{4}
6	2.38×10^{-4}	0.39 ± 0.004	5.5×10^{3}

It is interesting to note from Fig. 1b that extended state conduction range is more and more towards low temperature side as the lead concentration increases. This may be explained due to smaller activation energy of samples having higher concentration of lead where contribution of extended state conductivity will be larger as compared to low concentration of Pb at lower temperatures. The localized state conduction will therefore be predominant only at much lower temperatures at high concentration of Pb as compared to sample having lower concentration of Pb.

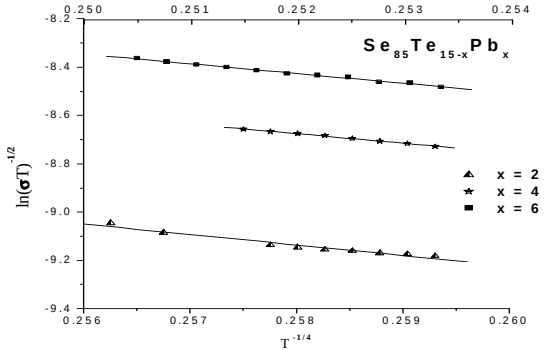

Fig. 2. $\ln(\sigma T^{1/2})$ vs. $T^{-1/4}$ plot at various concentration of Pb in a- $Se_{85}Te_{15-x}Pb_x$ system. The upper x-axis is plotted for x = 6.

In the low temperature region, data is plotted in Fig. 2 in terms of $\ln(\sigma T^{1/2})$ versus $T^{-1/4}$ to see the applicability of Mott's variable range hopping conduction model in our case. In such a case, the conduction can be attributed to the hopping of the charge carriers between localized states near Fermi level and the conductivity can be expressed as [15,16]:

$$\sigma T^{1/2} = \sigma_1 \exp(AT^{-1/4}) \quad (2)$$

$$\text{and} \quad A^4 = To = \lambda\alpha^3 / k\, N(E_F) \quad (3)$$

where $N(E_F)$ is the density of localized states at E_F, α^{-1} the degree of localization, T_0 the degree of disorder and λ and A are dimensionless constants. The value of pre-exponential term σ_1 of eq. as obtained by various workers is given by

$$\sigma_1 = 3e^2 \gamma [\, N(E_F) / 8\pi\alpha kT \,]^{1/2} \quad (4)$$

where 'e' is electron charge and the 'γ' Debye frequency ($=10^{13}$ Hz). A simultaneous solution of eq. (3) and (4) yields

$$\alpha = 22.52\sigma_0 A^2 (\text{cm}^{-1}) \quad (5)$$

$$\text{and} \quad N(E_F) = \sigma_1^3 A^2 (\text{cm}^{-3}\text{eV}^{-1}) \quad (6)$$

The hopping distance and hopping energy is given by

$$R = [9 / 8\pi\alpha kT\, N(E_F)]^{1/4} \quad (7)$$

$$W = 3/4\, \pi R^3 N(E_F) \quad (8)$$

$\ln \sigma T^{1/2}$ vs $T^{-1/4}$ plot is found to be a straight line which indicates the validity of hopping conduction mechanism (see Fig. 2). This is in good accordance with Mott's VRH model. The slope of these curves gives the value of N (E_F) and other Mott's parameters are calculated from eq. (2) - (8) and are given in Table 2. It is found that the value of T_0 decreases and α increases on increasing Pb concentration. Since T_0 represents the degree of disorder and α^{-1} the degree of localisation, it follows that the amorphicity of the sample decreases. It is evident from Table 2 that the density of localised states decreases as the percentage of lead increases in alloy. The hopping distance has been found to increase on increasing Pb concentration.

Table 2. Mott's Parameters in the low temperature region.

Pb_x (x at %)	A ($K^{1/4}$)	$T_0 \times 10^6$ (K)	σ_1(Ω^{-1} cm^{-1}K$^{1/2}$)	$N(E_F)$ (eV^{-1}cm^{-1})	$\alpha \times 10^5$ (cm^{-1})	R (cm)	W (eV)	αR
2	46.93	4.85	15	1.6×10^{17}	7.4	6.5×10^{-6}	.056	4.8
4	45.64	4.34	12	8.3×10^{16}	5.7	8.1×10^{-6}	.054	4.6
6	41.73	3.04	5.1	5.0×10^{15}	2.0	2.1×10^{-5}	.052	4.2

Thus from the experimental results in the present system, one can clearly see that the charge transport in the low temperature range can be attributed to the hopping of the charge carriers in the localized states near Fermi level. It may be mentioned here that the variable range of hoping conduction is not generally observed in chalcogenide glasses due to paired defect states. In spite of this, several researchers [17-19] have reported variable range hopping in chalcogenide glasses.

The study of transient photoconductivity measurements as a function of temperature and light intensity in a-semiconductors is a valuable tool in achieving a good understanding of the recombination process and distribution of localized states which control the photo-transport kinetics. Transient photoconductivity measurements are carried out by illuminating the thin films using unpolarised white light for 5 min. in the present case and recording the current simultaneously. Then, the light is turned off and the decay current is followed. The dependence of the photoconductivity response (the rise and relaxation section of the curve) on time in a- $Se_{85}Te_{15-x}Pb_x$ is presented in Fig. 3. This figure shows that the rise and fall sections of photoconductivity are asymmetric. The conductivity observed in rise and decay section also increases with the increase of Pb concentration in the alloy. The long photoconductivity rise time and slow decay process observed in the thin film is due to the presence of the deep localised gap states in these materials that behaves as trapping centers and recombination centers and increases with the increase of Pb concentration [20].

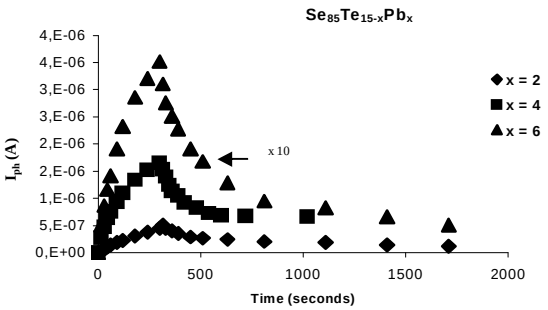

Fig. 3. Rise and decay of photoconductivity as a function of time in a- $Se_{85}Te_{15-x}Pb_x$.

The experimental data for the decay at different intensities for the case of a- $Se_{85}Te_{13}Pb_2$ in white light is plotted as a function of time in Fig. 4. It is clear from Fig. 4 that the behaviour of the decay curves is of the same nature at different intensities. Initially, the photocurrent decays fast and then becomes slow as time elapses.

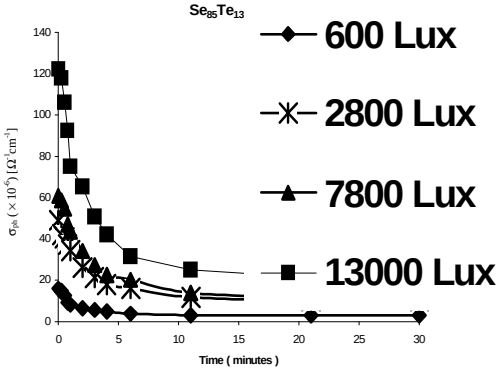

Fig. 4. Time dependence of photoconductivity at different intensities during decay at room temperature in a- $Se_{85}Te_{13}Pb_2$.

A persistent photocurrent is also observed which takes many hours to decay. The persistent photocurrent is found to be more when the samples are exposed to higher intensities (see Fig. 4). The results for other glasses were also of the same nature.

To observe the effect of temperature, measurements were also made at different temperatures keeping the intensity of light constant. The decay of photocurrent in this case is shown in Fig. 5. In this case also, the behaviour of the decay curves is similar at different temperatures except that the persistent photocurrent increases as temperature of measurement increases.

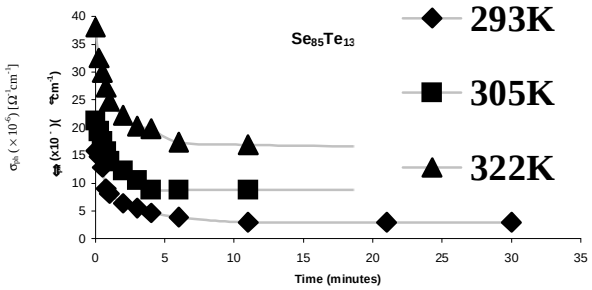

Fig. 5. Time dependence of photoconductivity at different temperatures at 600 Lux during decay in a- $Se_{85}Te_{13}Pb_2$.

The above results suggest that the persistent photocurrent is produced by some kind of defects that are accumulated during the illumination. From the decay curves, one has the impression that there are at least two decaying processes; namely, a very rapid one and an extremely slow one, which lead to the long tail in the decay curve.

Such types of long lived photocurrent have also been observed in other chalcogenide glasses [21-30] and it is believed that such a large decay constant can not be due to carriers trapped in the intrinsic defects [31] but may be due to some kind of structural changes on light shining which

are of reversible kind, i.e., they are removed on annealing at room temperature for longer times (a few days in some cases).

To understand the trapping effects, the persistent photo-conductivity is subtracted from the measured photo-conductivity, and then corrected photo-conductivity is plotted against time at different intensities at room temperature (293 K) in Fig. 6 respectively in case of a-$Se_{85}Te_{13}Pb_2$. Same results are obtained for other samples. From the logarithmic graph, one can conclude that the relaxation curve, in particular, is composed of two parts, the first one with a substantial decrease and the second one with a small slope. The part with a greater slope corresponding to the processes connected with trapping levels where as the part with a small slope corresponds to a recombination processes. At room temperature and higher temperature recombination processes are dominant.

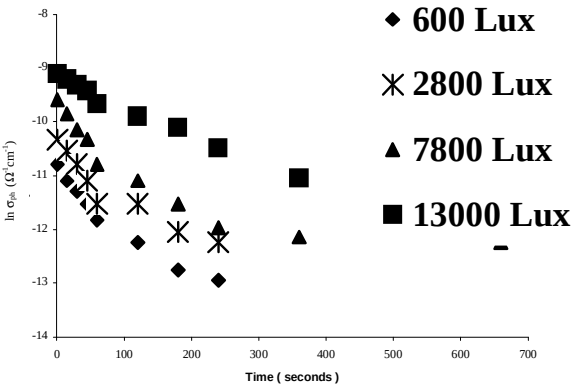

Fig. 6. Time dependence of photoconductivity at different intensities during decay in a-$Se_{85}Te_{13}Pb_2$ at room temperature after subtraction of persistent photoconductivity.

Fig. 8 depicts that the slow decay process is a function of time and can be described using the differential lifetime τd as used by Fuhs and Stuke [32]. The lifetime for such a slow decay process can be written as

$$\tau_d = [d (\ln \sigma_{ph}) / dt]^{-1} \quad (9)$$

where σ_{ph} is the maximum photo conductivity at t = 0 for a given temperature

In the case of exponential decay the differential lifetime will be equal to the carrier lifetime. However, in case of a non-exponential decay τ_d will increase with time and only the value at t = 0 will correspond to the carrier lifetime.

The decay time observed for the vacuum deposited a-$Se_{85}Te_{13}Pb_2$ thin film is found to be time dependent and the relation between ln τ_d and ln t is shown in Fig. 7. A straight-line graph is observed and this non-linear behaviour confirms the non-exponential decay process involved in a- $Se_{85}Te_{13}Pb_2$ thin film samples. The same behaviour is found in other samples in a- $Se_{85}Te_{15-x}Pb_x$ glassy alloy. For an exponential decay τ_d should be constant with time. This indicates that the traps exist at all the energies in the band gap, which have different time constant and hence giving the non-exponential decay of photo-conductivity.

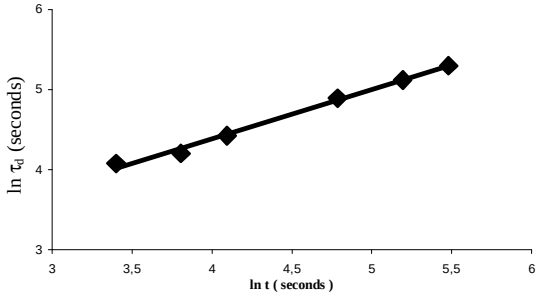

Fig. 7. A plot of ln τ_d versus ln t showing the non-exponential decay in a- $Se_{85}Te_{13}Pb_2$ thin film.

The extrapolation of the curve at lnt = 0, gives the value of the carrier lifetime and it is found to be 1.93 second in this case.

4. Conclusions

Electrical characteristics of a-$Se_{85}Te_{15-x}Pb_x$ thin film prepared by vacuum deposition technique have been studied. The conductivity measurements show that the d.c. conductivity increases on increase of Pb concentration. The activation energy calculated for the samples follow the same trend with Pb as with optical energy band gap. In the low temperature region, a- glassy system exhibits variable range hopping conduction and density of localized state calculated by Mott's VRH Model, decrease on increase Pb incorporation. The transient photoconductivity studied in the samples show non-exponential decay. Persistent current is also found in these samples and increase with increase of illumination and temperature. The differential lifetime is calculated. The photo decay process in a-$Se_{85}Te_{15-x}Pb_x$ films reveals the presence of deeper localised states and the carrier lifetime is found to be 1.93 second.

References

[1] J. Rowlands, S. Kasap, Physics Today **50**, 24 (1997).

[2] D. Drabold, X. Zhan, J. Li, "First principles molecular dynamics and photostuctural response in amorphous silicon chalcogenide glasses", WILEY-VCH Verlag Berlin GmbH, 9 October 2002.

[3] J. Mort, Physics Today **47**, 32 (1994).

[4] Ke. Tanaka, Phys. Rev. B 57 (1998) 5163; K. Tanaka, N. Yoshida, Sol. State Phen. **55**, 153 (1997).
[5] K. L. Bhatia, P. Singh, N. Kishore, S. K. Malik, Philos. Mag. **B 72**, 417 (1995).
[6] N. Kushwaha, N. Mehta, R. K. Shukla, D. Kumar, A. Kumar, J. Optoelectron. Adv. Mater. **7**(4), 2293 (2005).
[7] V. S. Kushwaha, N. Mehta, N. Kushwaha, A. Kumar, J. Optoelectron. Adv. Mater. **7**(4), 2035 (2005).
[8] N. Toghe, H. Matsuo, T. Minami, J. Non-cryst. Solids **96**, 809 (1987).
[9] K. L. Bhatia, D. P. Gosain, G. Parthasarathy, E. S. R. Gopal, S, K. Sharma, J. Mater. Sci. Lett., **51**, 181 (1986).
[10] S. K. Khan, M. Zulfequar, M. Hussain, Vacuum **72**, 291 (2004).
[11] S. Kohali, V. K. Sachdev, R. M. Mehra, P. C. Mathur, Phys. stat. sol. **209**, 389 (1988).
[12] N. B. Maharajan, N. S. Saxena, D. Bhandari, M. M. Imran, D. D. Paudyal, Bull. Mater. Sci. Vol. **23**(5), 369 (2000).
[13] M. S. Kamboj, G. Kour, R. Thangraj, Thin solid film **420**, 350 (2002).
[14] V. Pandey, N. Mehta, S. K. Tripathi, A. Kumar, J. Optoelectron. Adv. Mater. **7**, 2641 (2005).
[15] N. F. Mott, Philos. Mag. **22**, 7 (1970).
[16] N. F. Mott, E. A. Davis, Philos. Mag. **22**, 903 (1970).
[17] A. S. Maan, D. R. Goyal, S. K. Sharma, T. P. Sharma, Phys. III France **4**, 493 (1994).
[18] M. A. M. Khan, M. Zulfequar, M. Hussain, Physica B **322**, 1 (2002).
[19] M. A. M. Khan, M. Zulfequar, A. Kumar, M. Hussain, Mat. Chemistry and physics **87**, 179 (2004).
[20] N. Kushwaha, V. S. Kushwaha R. K. Shukla, A. Kumar J. Non-Cryst. Solids **351**, 3414 (2005).
[21] M. Dixit, S. K. Dwivedi, A. Kumar, Thin Solid Films **333**, 165 (1998).
[22] S. Singh, R. S. Sharma, R. K. Shukla, A. Kumar Vacuum **72**, 1 (2004).
[23] K. Shimakawa, A. Yoshida, T. Arizumi, J. Non-Cryst. Solids **16**, 258 (1974).
[24] S. Goel, A. Kumar, Thin Solid Films **151**, 307 (1987).
[25] E. A. Fagen, H. Fritzsche, Non-Cryst. Solids **4**, 480 (1970).
[26] J. F. Federici, D. M. Bubb, J. Superconductivity: Incoporating Novel Magnetism **14**, 331 (2001).
[27] Yeong-Ah Soh, G. Aeppli, F. M. Zimmermann, G. D. Isaacs, A. I. Frenkel, J. Appl. Phys. **90**, 6172 (2001).
[28] W. Wang, S. J. Chua, G. Li, J. Electronics Materials **29**, 27 (2000).
[29] H. M. Chen, Y. F. Chen, M. C. Lee, M. S. Feng, J. Appl. Phys. **82**, 899 (1997).
[30] X. Z. Dang, C. D. Wang, E. T. Yu, K. S. Boutros, J. M. Redwing, Appl. Phys. Lett. **72**, 2745 (1998).
[31] M. Igalson, Solid State Commun. **44**, 247 (1982).
[32] W. Fuhs, J. Stuke, Phys. Stat. Solidi **27**, 171 (1968).

* Corresponding author: dr_ashok_kumar@yahoo.com